Available online at www.sciencedirect.com

ScienceDirect

Procedia Materials Science 6 (2014) 1557 – 1565

Procedia Materials Science

www.elsevier.com/locate/procedia

3rd International Conference on Materials Processing and Characterization (ICMPC 2014)

Spray pyrolyzed $ZnSnO_3$ nanostructured thin films for hydrogen sensing

L.A. Patil[a,]*, I.G. Pathan[b], D.N. Suryawanshi[c], A.R. Bari[d], and D.S. Rane[e]

[a] *Nanomaterials Research Lab., Pratap College, Amalner 425 001, India*

[b] *Arts, Commerce and Science College, Navapur 425 418, India*

[c] *Rani Laxmibai College, Parola 425 111, India*

[d] *Arts, Commerce and Science College, Bodvad 425 310, India*

[b] *D.N Bhole College, Bhusawal 425 001, India*

Abstract:

Nanostructured $ZnSnO_3$ thin films were prepared onto preheated glass substrate by a spray pyrolysis technique using water soluble Zinc chloride and Stannic chloride as precursors. The crystallinity of the prepared samples was analyzed by X-ray diffraction spectroscopy. The X-ray diffractogram of as prepared thin film clearly indicated the stichiometric and pervoskite nanostructured nature of $ZnSnO_3$. The TEM image shows few nanorods along with fine particles of pervoskite $ZnSnO_3$. The band gap energy of thin film sample was observed to be 4.13eV. The band gap energy was found to be enhanced as compare to the reported value. The sample showed selective response to H_2 gas among the various gases such as LPG, hydrogen, ethanol, chlorine, carbon dioxide and ammonia. The dynamic response of $ZnSnO_3$ pervoskite thin film sample is presented. The pervoskite oxides were used as potential gas sensing material for their stability in thermal and chemical atmospheres.

Selection and peer review under responsibility of the Gokaraju Rangaraju Institute of Engineering and Technology (GRIET)

Keywords: Transparent conducting oxides, pervoskite thin films, spray pyrolysis, H_2 sensor, nanorod

1. Introduction

Lot of efforts are going on for hydrogen to supplant the hydrocarbons hence it may be possible to use hydrogen as the common fuel of the future. Basically it is an invisible, odorless and flammable gas, it is necessary to detect leakage of hydrogen in the environment. There is a strong need to develop novel hydrogen sensor for: solid oxide fuel cells, hydrogen engine cars, transportation and storage of hydrogen or other applications. Recently the main effort of hydrogen sensor development has been the improvement of hydrogen gas sensitivity and selectivity as

* Corresponding author. Tel.: +0-000-000-0000 ; fax: +0-000-000-0000 .
E-mail address: plalchand_phy_aml@yahoo.co.in

Selection and peer review under responsibility of the Gokaraju Rangaraju Institute of Engineering and Technology (GRIET)
doi:10.1016/j.mspro.2014.07.137

well. Compact, reliable, inexpensive and low power consumption sensor devices that can detect hydrogen have been subject of many research groups [Oleg Lupen et.al 2008].

Due to small size and the high surface-to volume ratio, nanostructured materials often exhibit novel and sometimes unusual properties [Edelstein et al 1996, Hadijipanyis et al 1994, Wang et al 2003]. The optical, electrical, thermal and chemical properties depend to a large extention the particle size and shape of these materials [Edelstein et.al 1996, Hadijipanyis et.al 1994, Wang et al 2003]. The large number of surface and edge atoms provides active sites for catalyzing surface reactions. In the area of chemical and gas sensitive semiconductor devices and nanoelectronics, ZnO, SnO_2 and their composites are finding great interest and attention in recent years [Edelstein et al 1996, Hadijipanyis et al 1994, Wang et al 2003]. Nowadays, nanostructured materials such as semiconducting metal oxide nanoparticles, nanowires and nanorods have been widely used for gas-sensing applications. Zinc oxide (ZnO) and Tin dioxide (SnO_2) are n-type semiconductors of wurtzite and rutile crystal structures respectively. They have wide band gaps 3.2-3.43 eV and 3.6-3.97 eV respectively [Fouad et al 2008]. SnO_2 is a promising material for gas-sensing applications due to its suitable physicochemical properties including high response, high stability, reactivity to reducing gases such as hydrogen and also low production cost [Demarne et al 1992, Naral et.al 2000, Mukhopadhyay et al 2000, Safonova et al 2000, Kotsikau et.al 2004, Ivanoc et al 2004, Teeramongkonrasmee et.al 2000, Patil et al 2007]. $ZnSnO_3$ is a perovskite-type oxide material. The data on the synthesis of $ZnSnO_3$ are ambiguous and contradictory and among the large studies of materials, the details on ternary oxide systems with spinel or perovskite structure have been rarely published [Hotovy et al 1998].

There has been considerable interest in recent years in nanostructured gas-sensing materials in thin film form [Chai et al 1996, De et al 1997, Liu et.al 1997, Alver et al 2007]. Perovskite materials display a wide range of properties that make them attractive for a variety of electrical ceramic applications. Many methods, including ultrasonic spray pyrolysis [Alver et.al 2007], thermal evaporation deposition [Cheng et al 2007, Klason et al 2006, Khomenkova et al 2007], chemical vapor deposition [Su et al 2006], hydrothermal synthesis [Lupen et al 2007, Huang et al 2007, Kale et al 2007, Kim et al 2006] and others [Kuo et al 2005, Du et al 2005], have been used to produce ZnO, SnO_2 nanoparticles. In this study, nanostructured $ZnSnO_3$ nanorod was synthesized by a simple Spray pyrolysis method.

2. Experimental

2.1.Preparation of nanostructured thin films

Nanocrystalline $ZnSnO_3$ thin films were prepared from 0.1M aqueous solution of zinc chloride ($ZnCl_4 \cdot 5H_2O$) and stannic chloride ($SnCl_4.5H_2O$) (Loba chem extra pure). The stock solution was delivered to nozzle with constant and uniform flow rate of 5 ml/minute using air as a carrier gas. The spray (mist) produced by nozzle was sprayed onto the glass substrates heated at 400 ± 5^0C. Various parameters such as nozzle-to-substrate distance, deposition time, flow rate of solution, deposition temperature and concentration of source solution were optimized to obtain highly textured thin films of good quality. The concentration and the volume ratio of Zinc chloride and Stannic chloride precursors are kept fixed as 0.1 M and 30:70 respectively. The thin film samples with this composition were referred as S1. As prepared thin films were annealed at 500 ^{0}C for 1 hour in an air medium. Thin films (S1) was found to be the pervoskite $ZnSnO_3$. The film was found to be transparent and nanostructured in nature. Electrical and gas sensing properties of the film was tested for different gases as LPG, hydrogen, ethanol, carbon dioxide, chlorine and ammonia.

The possible reaction for the product may be given as

$$ZnCl_4.5H_2O + SnCl_4.5H_2O \rightarrow ZnSnO_3 + 6\ H_2O + 4\ H_2 \uparrow + 4\ Cl_2 \uparrow$$

3. Material characterizations

As prepared films were characterized by X-ray diffractometer (Philips PW 1730) using CuKα (λ = 1.5418 Å) radiation. The surface morphology and microstructure of the thin films were studied using Transmission electron microscope [CM 200 Philips (200 kV HT)]. The quantitative elemental analysis of the films was estimated by computer controlled energy dispersive X- ray analyzer (model JEOL JSM-6360 Å) attached to the scanning electron microscope. Absorption spectroscopy is used to determine the band gap energy of the samples. Electrical and gas sensing properties were measured using a static gas sensing system. The sensor performance on exposure of LPG, carbon dioxide, hydrogen, ammonia, ethanol and chlorine was tested.

3.1. Thickness measurement

The thickness of thin films S1 was measured by using Surface Profiler (Veeco Dektak- 150) having vertical resolution of $1.5A^0$, Lateral resolution of 100 nm and Lateral length of 200 nm. The thickness and roughness of sample S1 was found to be 27 nm and 135 nm respectively.

3.2 Crystal structure using X-ray diffraction

XRD patterns of the samples calcined at 500 ^{0}C with ratio of Zn:Sn as 30:70 is shown in figure 1. The reflections recorded of sample S1 can be readily indexed to pervoskite $ZnSnO_3$ [JCPD#28-1486]. It reveals from XRD that the films are polycrystalline in nature. The strongest peak observed at 26.5^0 can be attributed to the (100) plane of the face exposed hexahedron $ZnSnO_3$. The grain size is measured by measuring the width of the line of the widest diffraction peak. The average grain size of sample S1 was calculated by using Scherer equation (1) and i.e. 20 nm.

$d = 0.9\,\lambda / 2\beta \cos\theta$, where β = Full width at half of its maximum intensity and λ= wavelength.

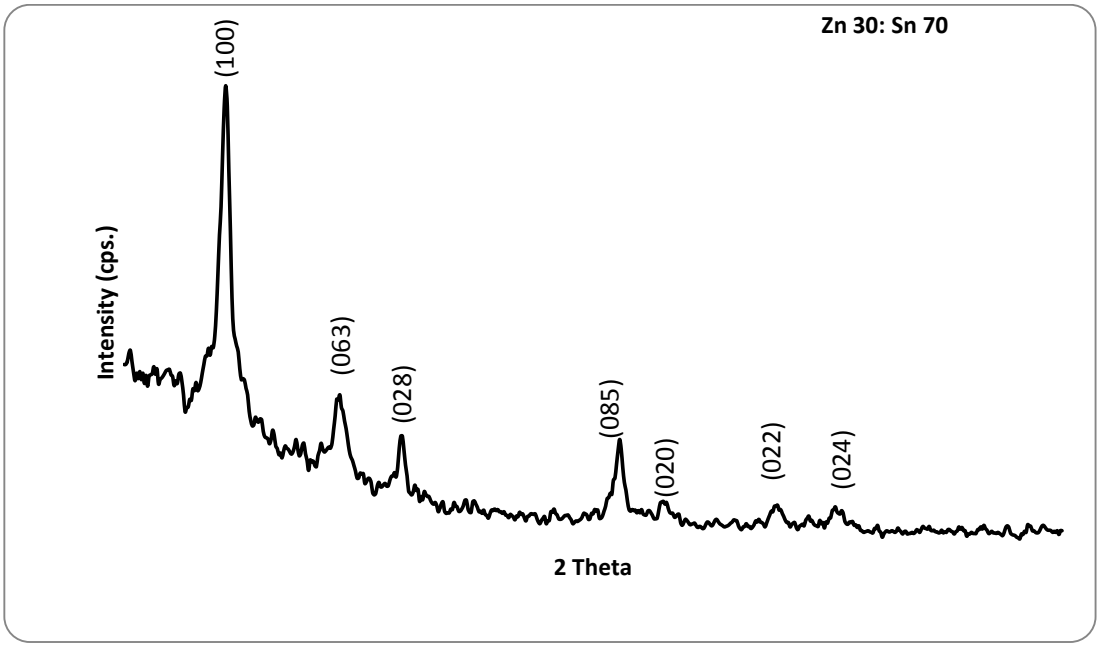

Fig. 1. X-ray diffractogram of nanocrystalline $ZnSnO_3$ pervoskite thin film

3.3. Quantititive elemental analysis (EDAX)

Table 1: The composition of pervoskite thin films

Sample No.	$ZnCl_4.5H_2O$ (ml)	Addition of $SnCl_4 \cdot 5H_2O$ (ml)	Mass % Zn	O	Sn
S1	30	70	18.56	61.76	19.68

It is clear from the table that the pervoskite thin films are stoichiometric in nature. The expected values of Zn, O and Sn are 20, 60 and 20 respectively. However there is little deviation from stoichiometry of the prepared film.

4 Microstructural analysis

4.1 Scanning electron microscopy

The microstructure and chemical composition of the film were analyzed by computer controlled energy dispersive X- ray analyzer attached to the scanning electron microscope (model JEOL JSM-6360 Å). Fig. 2(a) depicts SEM image of nanostructured S1 thin film sample. Scanning electron microscope could not resolve nanoparticles associated with the film even at very high magnification of "10E+5". It may be due to very small nanocrystalline particles associated with the film

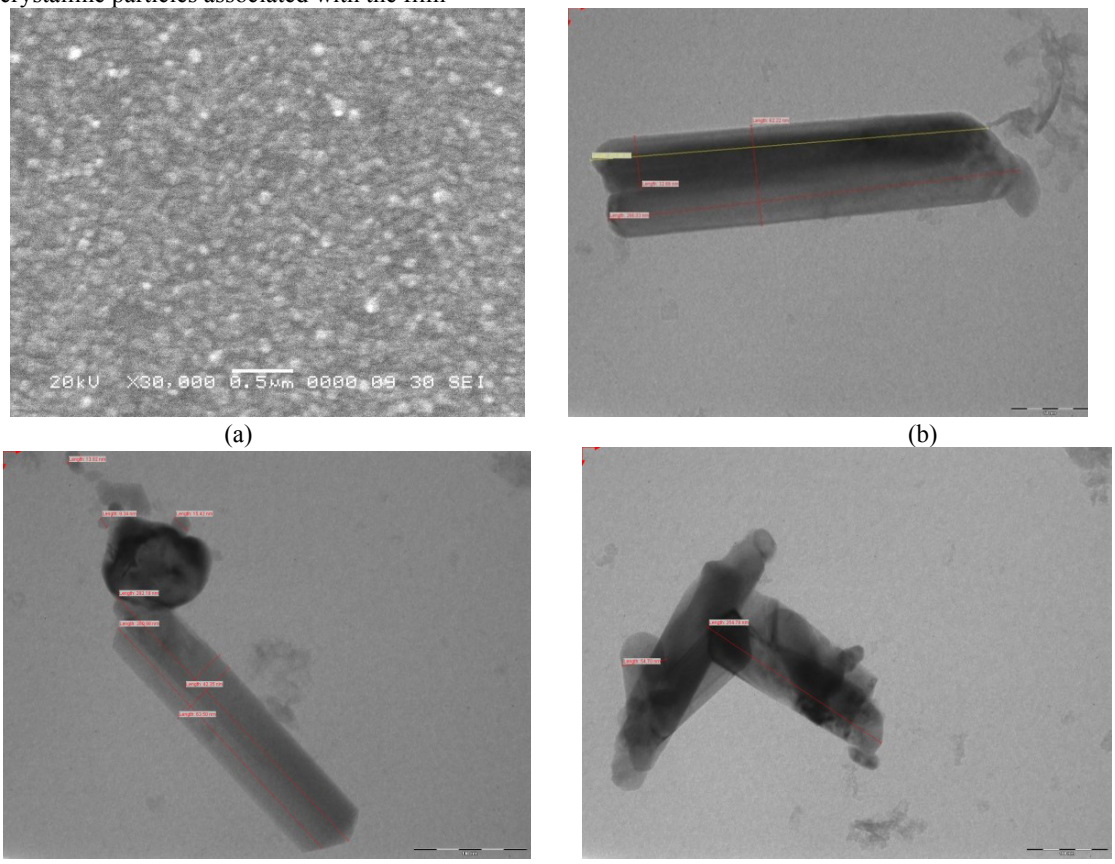

Fig.2 (a) SEM image, (b-d) TEM image of $ZnSnO_3$ pervoskite nanorod of $ZnSnO_3$ pervoskite thin film

4.2. Transmission electron microscopy

The image represented in fig.2(b-d) are TEM [CM 200 Philips (200 kV HT)] micrographs of $ZnSnO_3$ powder obtained from scratching the films synthesized at 400^0C. Powder consists of fine nanoparticles with few nanorods. The interaction between the gases and the sensitive layer is limited to the surface itself [Simon et.al 2001]. This is one of the reasons that nanostructured films give high gas response.

5. Optical properties

Figure 3 shows the absorbance spectrum of nanostructured pervoskite ZnSnO3 thin film. The absorbance of pervoskite $ZnSnO_3$ thin film sample (S1) was found to be with broad peak. The band gap energy of the sample was calculated from the absorption edges of the spectra [Bari et.al 2006]. The band gap energy calculated from absorbance spectra is 4.13 eV for sample S1. Reported band gap of ZnO is 3.2-3.43 eV and for SnO_2 it is 3.6-3.97 eV. The band gap of $ZnSnO_3$ was observed to be enhanced as compare to the reported band gap of ZnO and SnO_2. The increased band gap of the sample as compared to the reported value may be due to nanocrystalline nature of the

particles associated with the film.

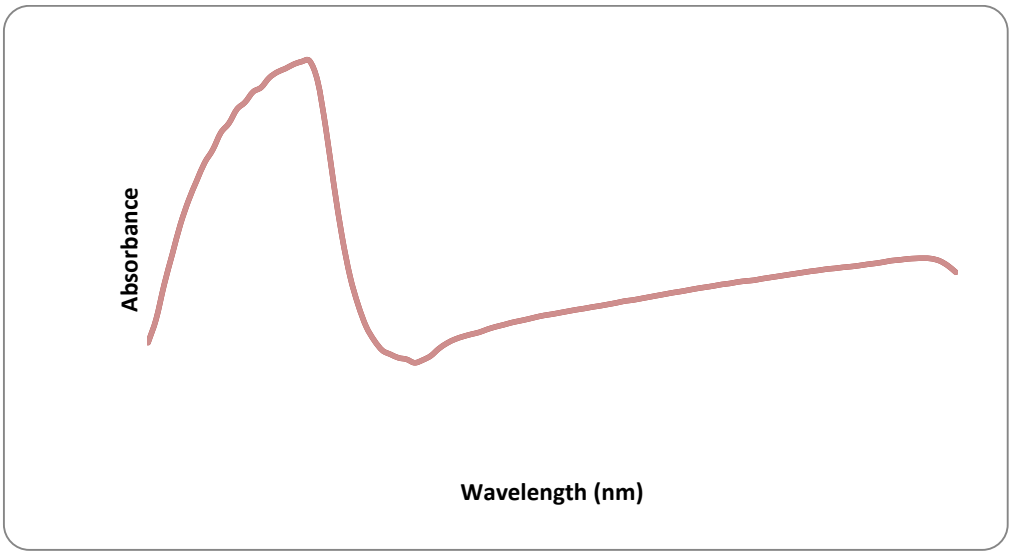

Fig. 3: Absorbance spectra of thin film samples S1.

6 Gas sensing performance of sensor

6.1 Measurement of gas response

Gas response (S) of the sensor was determined using the relation (2)

$$S = \frac{Gg - Ga}{Ga} \quad \text{---------- (2)}$$

where Ga and Gg are the conductances of substance in air and in a target gas medium, respectively. The time taken for the sensor to attain 90% of the maximum increase in conductance on exposure of the target gas is known as response time. The time taken by the sensor to get back 90% of the maximum conductance when the flow of gas is switched off is known as recovery time.

6.2 Gas response with operating temperature

Fig. 4 depict the variation of gas response with operating temperature of most sensitive nanostructured pervoskite $ZnSnO_3$, based sensor for all the gases under test. It is clear from figure that the nature of gas responses is similar for all gases. The response of H_2 gas goes on increasing with operating temperature, reaches to maximum (112.93) at 350^0C and decreases with the further increase of operating temperature. Response to a gas is related generally to the number of oxygen ions adsorbed on the surface of film. The species O^- or O^{2-} would have available largely on the $ZnSnO_3$ surface at 350^0C and hydrogen gas would have been oxidized quickly at this temperature to give higher sensitivity. Hence the response for hydrogen would have been maximum.

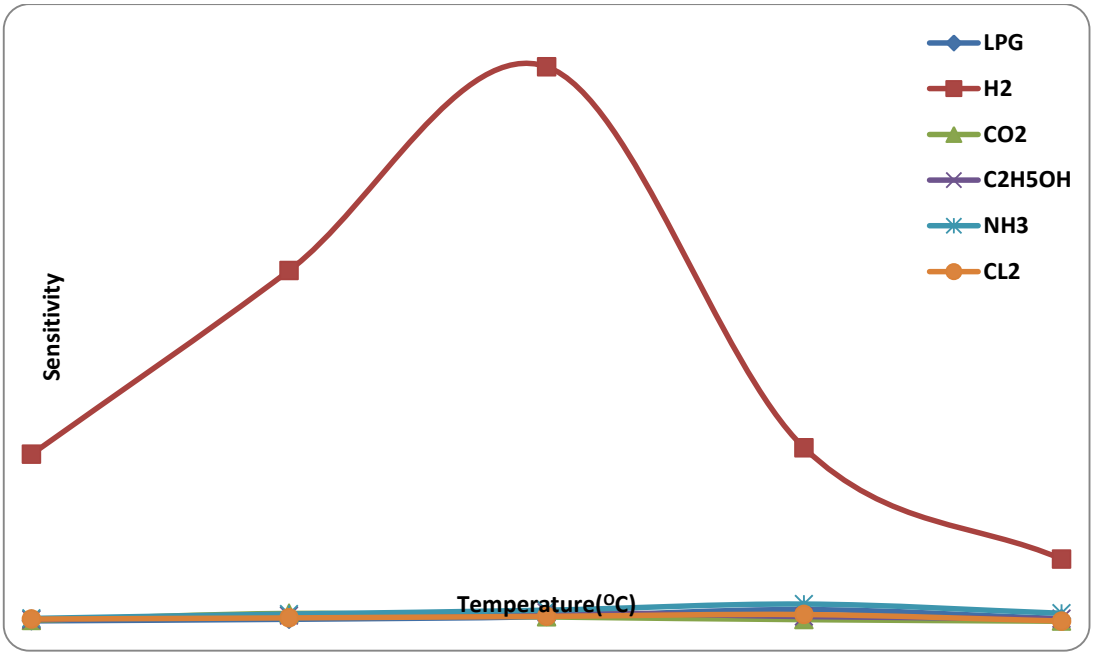

Fig. 4: Response of sensor S1 (Pervoskite ZnSnO3)

Table 2 : Comparison of hydrogen response of nanostructured based sensors

Nanomaterial	Method/form	H_2 response	Concentration (ppm)	Operating temperature(^{0}C)	Reference
$ZnSnO_3$	Spray pyrolysis/ thin film	112	1000	350	Present work
SnO_2	R.F magnetron Sputtering/thin film	300	500-10000	550	[33]
SnO_2	Hydrothermal route/ Thin film	11.9	1000	300	[34]
SnO_2	Ultrasonic spray pyrolysis/thin film	60	1000	350	[35]
ITO	R.F magnetron Sputtering/thin film	0.008	1000	300	[36]
$ZnSnO_3$	Hydrothermal route/ Thin film	2	1000	350	[37]

Table 2 presents comparison of hydrogen sensor between reported sensors of different materials [Niranjan et.al 2005, Kim et.al 2009, Hieda et.al 2008, Yoo et.al 2005, Xu et.al 2006] and nanostructured ZnSnO3 thin films (nanorod) in present investigation. It is clear that response of sensor reported in the present article is extremely high as compare to reported sensors.

6.3 Selectivity

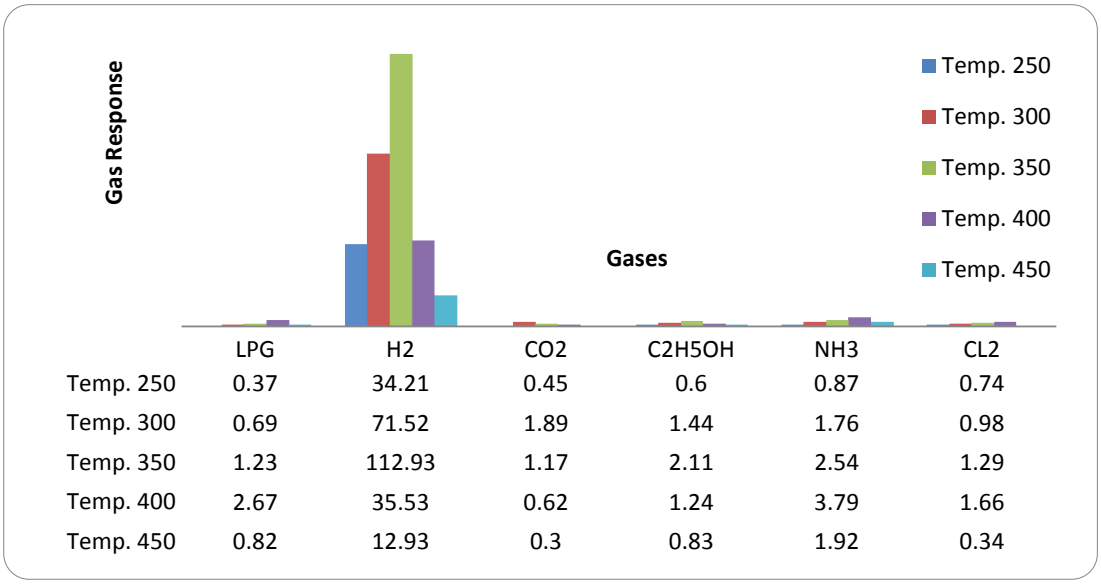

	LPG	H2	CO2	C2H5OH	NH3	CL2
Temp. 250	0.37	34.21	0.45	0.6	0.87	0.74
Temp. 300	0.69	71.52	1.89	1.44	1.76	0.98
Temp. 350	1.23	112.93	1.17	2.11	2.54	1.29
Temp. 400	2.67	35.53	0.62	1.24	3.79	1.66
Temp. 450	0.82	12.93	0.3	0.83	1.92	0.34

Fig. 5: Histogram showing selective response of hydrogen among various gases as a function of temperature.

Figure 5 depicts the selectivity of H_2 gas in comparison with all other gases tested at 350^0C. It is clear from histogram that the sensor is highly selective to hydrogen gas against other gases.

6.4 Response and recovery profile of sample S1, S3 and SF2

The time taken for the sensor to attain 90% of the maximum decrease in the resistance on exposure to the target gas is the response time. The time taken for the sensor to get back 90% of its original resistance is the recovery time. The transient response of nanostructured pervoskite $ZnSnO_3$ sample S1 for hydrogen is presented in figure 6. For the samples S1 quick response time was observed to be 8 second and recovery time was 12 second. The thin film sensor showed quick response and fast recovery. This may be possible due to nanocrystalline nature of the film.

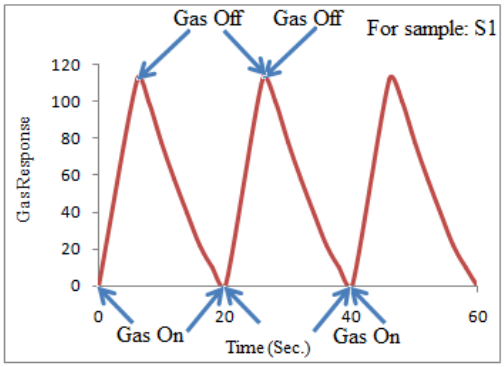

Figure 6: Response and Recovery of sample of S1

7. Discussion

The properties of nano- and microcrystals depend not only on their composition, but also on their structure, phase, shape, size and size distribution. The reactivity and selectivity of a nanocatalyst can be tailored by controlling the shape, as it will determine the crystallographic facets exposed on the surface of a nanocrystal and therefore the number of atoms located at the edges or corners. Besides the activation of the crystallographic facets exposure to target gases, high surface to volume ratio is also crucial. However, high surface to volume ratio can be obtained not only by reducing grain size, but also by highly-ordered pore structure such as mesoporous structure or nanotube arrays or nanorods. However the most of such structured materials are not stable after the removal of surfactant and

pore structure would collapse at high temperature [Ciesla et.al 1994, Hudson et.al 1996].

The adsorption-desorption sensing mechanism can be explained on the basis of reversible chemisorptions of the hydrogen on the pervoskite $ZnSnO_3$ nanorod. It produces a reversible resistivity change with exchange of charges between hydrogen and $ZnSnO_3$ surface leading to change in the depletion width [Hartnagel et.al 1995]. One of the intuitive effects in sensitivity improvement is due to the change in the surface to volume ratio. It is a well known fact that oxygen would be adsorbed on a $ZnSnO_3$ nanostructured particles as O_2^-, O^- and O^{2-} ions by extracting electrons [Lupen et.al 2008] from the conduction band. Gas sensing is based on interaction between the negatively charged oxygen adsorbed on the $ZnSnO_3$ surface and hydrogen to be detected. Initially molecular oxygen are adsorbed on the surface of $ZnSnO_3$ nanoparticles and electrons are consumed following the reactions:

$$O_2(gas) \leftrightarrow O_2(ads) \leftrightarrow O_2(ads) + e^- \leftrightarrow O_2^-(ads)$$

thus increase of the nanostructured film resistance. When the nanostructured $ZnSnO_3$ sensor is exposed to a reducing test gas hydrogen, its atom react with these chemisorbed oxygen ions and produce H_2O molecules consuming chemisorbed oxygen from film surface by releasing electrons. The sensing mechanism for hydrogen may be represented by following reaction:

$$(O^-)_{ZnSnO3} + 2H \rightarrow H_2O(g) + e^-$$

$$2H_2 + O_{2\,(ads)}^- \rightarrow 2H_2O + e^-$$

considering $O^{2-}_{(ads)}$ as the predominant adsorbed species on $ZnSnO_3$ film surface, the electrons will be released back to the conduction band and will contribute to increase in the current through a nanorod. This also results in a reduction of surface depletion width and increase conductivity. The reaction is exothermic in nature [Lupen et.al 2008] and the molecular water desorbs quickly from the surface.

Conclusions

1. Nanostructured pervoskite $ZnSnO_3$ thin films were successfully prepared by simple spray pyrolysis technique.
2. The microstructural and morphological properties of samples showed the nanostructured particles and rod in the film .
3. The band gap energy of S1 samples was observed to be 4.13 eV. The band gap of $ZnSnO_3$ was observed to be enhanced (4.13eV) as compared to the reported band gap (3.6 eV). It may be due to nanocrystalline nature of the film.
3. The pervoskite $ZnSnO_3$ nanostructured film showed selective response to hydrogen gas as compared to other gases.

Acknowledgements

The authors are thankful to the Head, Department of Physics and Principal Prof. Dr. L.A.Patil, Pratap College, Amalner for providing laboratory facilities for this work.

References

Alver U., Kilinc, T. E. Bacaksiz, T. Kuecuekoemeroglu, S.Nezir, I. H. Mutlu, F. Aslan, *Thin Solid Films*, 515 (2007) 3448-3451.
Bari R.H., Patil L.A. and Patil P.P., Bull. Mater. Sci., 29 (2006) 529. Basic Research Needs to Assure a Secure Energy Future, A Report from the Basic Energy Sciences Advisory Committee, February 2003, available from: <http://www.sc.doe.gov/bes/besac/Basic_Research_Needs_To_Assure_A_Secure_Energy_ Future_FEB2003.pdf>.
Chai C. C., Peng J., Yan B. P., *Sens. Actuators B,* 34 (1996) 412-416.
Ciesla U., Demuth, D. Leon, Petroff R., Stucky P., Unger, G., Schuth K. F., *Surfactant Chem. Commun,* (1994) 1387-1388.
Cheng H. B., Cheng J. P., Zhang Y. J., Wang Q. M., *J. Crystal Growth,* 299 (2007) 34- 40.
De la M., Olvera L., Asomoza R., *Sens. Actuators B,* 45 (1997) 49-53.
Demarne V., Sanjine R., Sberveglieri G., *Kluwer Academic Publishers, Netherlans,* (1992) 89-116.
Du J. M., Liu Z. M., Huang Y., Gao Y. N., Han B. X., Li W. J., Yang G.Y., *J. Crystal Growth*, 280 (2005) 126-134.
Edelstein A. S., Cammarata RC, *Nanomaterials, Bristol*, (1996).
Fouad O. A., Glasspell G., El-Shall M.S., *Top Catal,* 47 (2008) 84-96.
Hadijipanyis G. C., Siegel R. W., *Kluwer Academic Publications, Nanophase materials, London* (1994).
Hieda K., Hyodo T., Shimizu Y., Egashira M., Sens. Actuators, B 133 (2008) 144–150.
Hotovy J., Bue D., Hascik S., Nennewitz O., *Vacuum,* 50 (1998) 41-44.
Huang Z.Y., Chai C.F., Cao B.Q., *Crystal Growth,* (2007) 1686-1689.
Hudson M. J., Knowles J. A., *J. Mater. Chemistry,* 6 (1996) 89-95.

Hartnagel H. L., Dawar, A. L., Jain A. K., Jagadish C., *IOP, Bristol,* (1995).
Ivanoc P., Llobet E., Vilanova X., Brezmes J., Hubalek J., Corrig X., *Sens. Actuators B*, (2004) 201-206.
Kandasami Asokan, Jae young park, Sun-woo Choi, Sang Sub Kim, *Nanoscale Res. Lett,* 5 (2010) 47-752.
Kale R. B., Lu, S.Y., J. *Phys. Condense Matter*, 19 (2007).
Kim H.R., Choi K.I., Lee J.H., Akbar S.A., Sens. Actuators, B 136 (2009) 138–143.
Kim Y. J., Lee C.H., Hong Y.J., Yi G.C., Kim S. S., Cheong H., *Applied Phys. Lett.,* 89 (2006) 63128-163128.
Kuo C. L., Kuo T.J., Huang M. H., *J. Phys. Chem. B,* (2005) 20115-20121.
Kotsikau D., Ivanovskaya M., Orlik D., Falasconi M., *Sens. Actuators B*, 101 (2004*)* 199-206.
Klason, P. K. Magnusson, O. Nur, Q.X. Zhao, Q.U.Wahab, M. Willander, *Phys. Scripta*, 126 (2006) 53-56.
Khomenkova L., Fernandez P., *Crystal Growth*, (2007) 836- 839.
Lupan O., Chow L., Chai G.Y., Roldan B., Naitabdi A., Schulte A., Heinrich H., *Mater. Science Eng. B*, 145 (2007) 57- 66.
Liu X.Q., Tao S.W., Shen Y.S., *Sens. Actuators B,* 40 (1997) 161-165.
Mukhopadhyay A. K., Mitra P., Chatterjee A. P., Maiti H. S., *Ceram. Int.*, 26 (2000) 123-132.
Nayral C., Viala E., Collière V., Fau P., Senocq F., Maisonnat A., Chaudret B., Appl. *Surf. Science,* 164 (2000) 219-226.
Niranjan R.S., Hwang Y.K., Kim D.K., Jhung S.H., Chang J.S., Mulla I.S., Mater. Chem. Phys. 92 (2005) 384–388.
Oleg Lupen, Guangyu Chai, Lee Chow, Microelectronic Engineering 85 (2008) 2220-2225.
Patil S.A., Patil L.A., Patil D. R., Jain G. H., Wagh M.S., *Sens. Actuators B,* 123 (2007) 233-239.
Safonova O.V., Rumyantseva M. N., Ryabova L. I., Labeau M., Delabouglise G., Gaskov A. M., *Material Science Eng., B, Solid State Mater. Advance Technol.,* 85 (2000) 43-49.
Su F. H., Wang W.J., Ding K., Li G. H., Liu Y.F., Joly A. G., Chen, W. *J. Phys. Chem. Solids,* 67 (2006) 2376-2381.
Simon I., Barson N., *Sens. Actuators B*, 73 (2001) 1-26.
Teeramongkonrasmee A., Sriyudthsak M., *Sens. Actuators B*, 66 (2000) 256-259.
Wang Z. L., *Kluwer Academic Publisher,* vol. I (2003).
Wang Z. L., *Kluwer Academic Publisher,* vol. II (2003).
Xu J., Jia X., Lou X and Shen J., Solid State Electron. 50 (2006) 504.
Yoo K.S., Park S.H., Kang J.H., Sens. Actuators, B 108 (2005) 159-164.